

# Exact Thermodynamics of Pairing and Charge-spin Separation Crossovers in Small Hubbard Nanoclusters

Armen N. Kocharian

*Department of Physics and Astronomy,  
California State University, Northridge,  
CA 91330-8268*

Gayanath W. Fernando

*Department of Physics, University of Connecticut,  
Storrs, CT 06269 and IFS, Hantana Rd., Kandy, Sri Lanka*

Tun Wang and Kalum Palandage

*Department of Physics, University of Connecticut,  
Storrs, CT 06269*

James W. Davenport

*Computational Science Center,  
Brookhaven National Laboratory,  
Upton, NY 11973*

The exact numerical diagonalization and thermodynamics in an ensemble of small Hubbard clusters in the ground state and finite temperatures reveal intriguing insights into the nascent charge and spin pairings, Bose condensation and ferromagnetism in nanoclusters. The phase diagram off half filling strongly suggests the existence of subsequent transitions from electron pairing into unsaturated and saturated ferromagnetic Mott-Hubbard like insulators, driven by electron repulsion. Rigorous criteria for the existence of quantum critical points in the ground state and corresponding crossovers at finite temperatures are formulated. The phase diagram for  $2 \times 4$ -site clusters illustrates how these features are scaled with cluster size. The phase separation and electron pairing, monitored by a magnetic field and electron doping, surprisingly resemble phase diagrams in the family of doped high  $T_c$  cuprates.

PACS numbers: 65.80.+n, 73.22.-f, 71.10.Fd, 71.27.+a, 71.30.+h, 74.20.Mn

## I. INTRODUCTION

Despite tremendous experimental and theoretical efforts, there is still no microscopic theory that can yield comprehensive support for the bare Coulomb interaction originated pairing correlations, phase separation and pseudogap phenomena in clusters, small nanoparticles, transition metal oxides and high  $T_c$  cuprates [1, 2, 3, 4, 5, 6, 7, 8, 9, 10]. The recent discovery of the ferromagnetic insulators at room-temperature has further stimulated a great interest related to the role of on-site Coulomb interaction in the origin of ferromagnetism [11]. Electrons in a finite Hubbard lattice, subjected to strong on-site electron repulsion near half filling, can lead to spontaneous ferromagnetism [12] and the finite temperature phase diagram is expected to be applicable to disulfides [13]. Moderate Coulomb interaction can also lead to phase separation and formation of mesoscale structures (such as "stripes") under doping of Mott insulating "parent" materials with highly correlated electrons, including high  $T_c$  cuprates [14, 15, 16, 17]. Although the experimental determination of various inhomogeneous phases in the cuprates is still somewhat controversial [15, 16], the underdoped high  $T_c$  superconductors (HTSCs) have many common features and are of

ten characterized by crossover temperatures below which excitation (pseudo)gaps in the normal-state are seen to develop [17]. The detailed manner in which  $T_c$  and crossover temperature changes under variation of electron concentration, magnetic field or pressure (Coulomb interaction) is also of fundamental interest for the formulation of the microscopic models responsible for nascent superconductivity [18]. In the optimally doped cuprates, the correlation length of dynamical spin fluctuations is very small [19] and hence short-range fluctuations are dominant over long-range ones. Therefore, a microscopic theory, with short-range dynamical correlations, can give useful insight into nascent superconductivity in clusters and the rich physics observed in the high- $T_c$  cuprates. In our opinion, thermodynamic properties of small Hubbard clusters under variation of composition, size, structure, temperature and magnetic field have not been fully explored, although there have been numerous exact calculations [20, 21]. From this perspective the exact diagonalization of small Hubbard *nanoclusters* can give insights related to the origin of superconductivity and ferromagnetism in an ensemble of clusters, nanoparticles, and eventually, nanomaterials [22, 23].

The following questions are central to our study: (i) Using exact cluster studies, is it possible to obtain a mi-

croscopic understanding of charge and spin separation and electron charge pairing and identify various possible incipient phases at finite temperatures? (ii) Is it possible for ferromagnetism to occur in Mott-Hubbard like insulators away from half filling? (iii) Do these *nanocluster* phase diagrams retain important features, such as quantum critical points and crossovers that are known for mesoscopic structures and large thermodynamic systems? (iv) When treated exactly, what essential features can the simple Hubbard clusters capture that are in common with the transition metal oxides, cuprates, etc.?

In addition, 4-site (square) cluster is the basic building block of the CuO<sub>2</sub> planes in the HTSCs and it can be used as a block reference to build up larger superblocks in 2D of desirable  $L \times L$  sizes [24, 25, 26, 27, 28]. Short range electronic correlations provide unique insight into the Nagaoka ferromagnetism in small 2D and 3D ferromagnetic particles [12, 13], exact thermodynamics of many-body physics, which are difficult to obtain from approximate methods [22]. Here we present also strong evidence underlining the occurrence of saturated and unsaturated ferromagnetism [29], particle-particle, particle-hole *pairings* and corresponding temperature driven Bose condensation (BC) *crossovers* for spin and charge degrees in mesoscale structures.

The paper is organized as follows. In the following section we present the model and formulate exact thermodynamics in grand canonical ensemble approach. In the third section, we introduce the charge and spin pseudogaps and define corresponding new order parameters. In section four, we present the results of numerical calculations for electron density and magnetization versus chemical potential and illustrate how to calculate various phase boundaries for particle-particle/hole pairing, phase separation instabilities, quantum critical points in the ground state and crossovers at finite temperatures. The results for the  $2 \times 4$  cluster are used to illustrate how these features are scaled with the cluster size. The concluding summary is presented in the closing section.

## II. MODEL AND FORMALISM

The quantum and thermal fluctuations of electrons in finite clusters can be described by the Hubbard Hamiltonian, placed in a magnetic field  $h$  as,

$$H = -t \sum_{\langle ij, \sigma \rangle} c_{i\sigma}^+ c_{j\sigma} - \mu \sum_{i, \sigma} n_{i\sigma} + \sum_i U n_{i\uparrow} n_{i\downarrow} - h\gamma \sum_{i\sigma} (n_{i\uparrow} - n_{i\downarrow}), \quad (1)$$

with the hopping amplitude  $t$  (energies are measured in the units of  $t$ ) and on-site Coulomb interaction  $U \geq 0$ . Here  $\gamma = \frac{1}{2}$  is the magnetic moment of an electron and  $\mu$  is the chemical potential for the ensemble of clusters. This work utilizes *statistical* canonical and grand canonical ensembles using analytical eigenvalues for 4-site clus-

ters with periodic boundary conditions [23]. In addition, here we present the results of exact numerical diagonalization of  $2 \times 4$  square 2D clusters, using numerical eigenvalues in the above ensembles to study thermal and quantum *fluctuations*.

In nanoparticles electrons and holes are limited to small regions and an effect known as quantum confinement yields discrete spectrum and energy-level spacings between filled and empty states that can modify the thermodynamics. Because the small clusters are far from thermodynamic limit, one can naively think that the standard tools for the description of phase transitions are not applicable and other concepts are needed. However, it is important to realize that phase transitions and corresponding temperature driven crossovers in the grand canonical ensemble can very well be defined and classified for finite systems without the use of the thermodynamic limit. It is further shown also how spatially inhomogeneous configurations like phase separations can be obtained using the canonical ensemble. We illustrate how phase transitions on the verge of an instability and phase separation (segregation) can be defined and classified unambiguously in finite Hubbard clusters [23]. It is thus possible to define phase transitions and crossovers even in small systems with local Coulomb forces, which are not thermodynamically stable. There is also strong support with regard to the effectiveness of the grand canonical approach for studies of magnetism in small clusters due to recent experimental findings that average magnetization of a ferromagnetic cluster is a property of the ensemble of isolated clusters but not of the individual cluster [1, 2].

One can eliminate next nearest neighbor couplings by replacing the planar square lattice with independent 4-site clusters and treat them as an ensemble immersed in a particle heat reservoir, where electrons can transfer from cluster to cluster due to the thermal fluctuations [23]. Earlier we formulated a new scheme in which thermodynamical/statistical notions, concepts and theoretical methodologies are tailored for the calculations of exact thermodynamics in a grand canonical ensemble of 4-site clusters. Degrees of freedom for charge and spin, electron and spin pairings, temperature crossovers, quantum critical points, etc. were extracted directly from the thermodynamics of these clusters [22, 23]. The grand partition function  $Z$  (where the number of particles  $N$  and the projection of spin  $s^z$  are allowed to fluctuate) and its derivatives are calculated exactly without taking the thermodynamic limit [22]. The charge and spin fluctuation responses to electron or hole doping level (i.e. chemical potential  $\mu$ ) and an applied magnetic field ( $h$ ) resulting in weak *saddle point* singularities (*crossovers*), which display clearly identifiable, prominent peaks in corresponding charge and spin density of states [23].

### III. CHARGE AND SPIN PSEUDOGAPS

We apply the grand canonical ensemble of decoupled clusters in contact with a bath reservoir allowing for the particle number to fluctuate. It is straightforward to calculate the above thermodynamic properties and some of these results for the 2- and 4-site clusters were reported earlier [22]. Using these eigenvalues, we have evaluated the exact grand partition function and thermal averages such as magnetization and susceptibilities numerically as a function of the set of parameters  $\{T, h, \mu, U\}$ . Using peaks in spin and charge susceptibilities, phase diagrams in a  $T$  vs  $\mu$  plane for arbitrary  $U$  and  $h$  can be constructed. This approach also allows us to obtain quantum critical points (QCPs) and rigorous criteria for various sharp transitions, such as the Mott-Hubbard (MH), antiferromagnetic (AF) or ferromagnetic (F) transitions in the ground state [22] and charge (particle-particle) or spin condensation at finite temperatures [23] using peaks in charge or spin susceptibilities (see below).

The difference in energies for a given temperature between configurations with various numbers of electrons is obtained by adding or subtracting one electron (charge) and defined as,

$$\Delta^c(T) = [E(M-1, M'; U, T) - E(M+1, M'; U, T)] - 2[E(M, M'; U, T) - E(M+1, M'; U, T)], \quad (2)$$

where  $E(M, M'; U, T)$  is the lowest canonical (ensemble) energy with a given number of electrons  $N = M + M'$  determined by the number of up ( $M$ ) and down ( $M'$ ) spins. The quantity  $\Delta^c(T)$  is related to the discretized second derivative of the energy with respect to the number of particles, i.e. charge susceptibility  $\chi_c$ . We define the chemical potential energies at finite temperature as  $\mu_{\pm}$ ,

$$\mu_+ = E(M+1, M'; U : T) - E(M, M'; U, T) \quad (3)$$

$$\mu_- = E(M, M'; U : T) - E(M-1, M'; U, T). \quad (4)$$

Eqs. (3) and (4) at  $T = 0$  are identical to those introduced in [30], near half filling. One usually refers to MH transitions, plateaus or gaps in  $\langle N \rangle$  vs  $\mu$ , as those occurring only at half filling  $\langle N \rangle = 4$  in the 4-site cluster with lower and upper Hubbard subbands separated by the energy gap. At half filling, one can recall MH and AF critical temperatures, at which corresponding MH and AF gaps disappear. Similar steps (gaps) at other  $\langle N \rangle$  in charge and spin degrees will be referred to as MH-like and AF-like plateaus respectively in order to distinguish these. This terminology would also apply to all the labelings in Fig. 1 and the rest of the paper. Using the definitions (3) and (4), the corresponding charge energy gap,  $\Delta^c(T)$ , at finite temperature can be written as a difference,  $\Delta^c(T) = \mu_+ - \mu_-$ . Notice that  $\mu_+(T)$  and  $\mu_-(T)$  identify peak positions in a  $T - \mu$  space for charge susceptibility  $\chi_c$  at finite temperature. The condition  $\Delta^c(T) > 0$  provides electron-hole (excitonic) excitations, with a positive pseudogap,

$\Delta^{e-h}(T) \geq 0$  [22]. Accordingly, the condition  $\Delta^c(T) < 0$  with  $\mu_-(T) > \mu_+(T)$  gives electron-electron pairing with positive energy,  $\Delta^P(T) > 0$  [23]. Using the above definitions for  $\mu_{\pm}$  we can combine them and write:

$$\Delta^c(T) = \begin{cases} \Delta^{e-h}(T), & \text{for } \mu_+ > \mu_- \\ \Delta^P(T), & \text{for } \mu_- > \mu_+, \end{cases} \quad (5)$$

where  $\Delta^{e-h}(T) \geq 0$  serves as a natural order parameter and will be called a MH-like *pseudogap* at nonzero temperature, since  $\chi$  has a small, but nonzero weight inside the gap at infinitesimal temperature. At  $T = 0$ , this gap will be labeled a true gap since  $\chi_c$  is exactly zero inside. For a given  $U$ , we define the crossover critical temperature  $T_c(U)$  at which the electron-hole pairing pseudogap vanishes and a Fermi liquid state, with  $\mu_- = \mu_+$ , becomes stable.

At zero temperature, the expression for electron binding energy  $\Delta^P(T)$  is identical to *true gap* introduced in Ref. [35] and at nonzero temperature it will be called a pairing pseudogap. We can easily trace the peaks of  $\chi_c(\mu)$  at *finite* temperature, and find  $T_c(\mu)$  at which a possible maximum occurs for a given  $\mu$ . At finite temperature, the charge susceptibility is a differentiable function of  $\mu$  and the peaks, *which may exist in a limited range of temperature*, are identified easily from the conditions,  $\chi_c'(\mu_{\pm}) = 0$  with  $\chi_c''(\mu_{\pm}) < 0$ . The charge pseudogap at half filling  $\mu_0 = \mu_+ = \mu_- = \frac{U}{2}$  vanishes at  $T_{MH}$  which can be identified clearly with  $\chi_c(\mu_0) = 0$  and  $\chi_c''(\mu_0) = 0$ ; i.e. as the temperature corresponding to a point of inflection in  $\chi_c(\mu)$ . This procedure describes rigorous conditions for identifying the MH transition temperature and a similar one can be carried out for the spin gap,  $\Delta^s(T)$ , by following the evolution of spin susceptibilities  $\chi_s(\mu)$  as a function of  $\mu$ . Possible peaks in the zero magnetic field spin susceptibility  $\chi_s(\mu)$ , when monitored as a function of  $\mu$ , can be used to define an associated temperature,  $T_s(\mu)$ , as the temperature at which such a peak exists and a spin pseudogap as the separation between two such peaks.

Similar to the charge plateaus seen in  $\langle N \rangle$  versus  $\mu$ , we can trace the variation of magnetization  $\langle s^z \rangle$  versus an applied magnetic field  $h$  and identify the spin plateau features which can be associated with staggered magnetization or short range AF. We calculate the critical magnetic field  $h_{c\pm}$  for the onset of magnetization which depends on  $U$ ,  $T$  and  $N$ , by flipping a down spin, or an up spin [23]. The difference in energies for given temperature between configurations with various spins defines the spin pseudogap

$$\Delta^s(T) = \frac{h_+ - h_-}{2}, \quad (6)$$

where  $h_+$  and  $h_-$  identify the peak positions in the  $h$  space for the spin susceptibility  $\chi_s$ . The condition  $\Delta^s(T) > 0$  yields spin (AF-like) paring,  $\Delta^{AF}(T) > 0$ , with a positive (spin) pseudogap [23]. Accordingly, the condition  $\Delta^s(T) < 0$  with  $h_-(T) > h_+(T)$  yields a ferromagnetic pairing pseudogap,  $\Delta^F(T) > 0$ , for spin (triplet

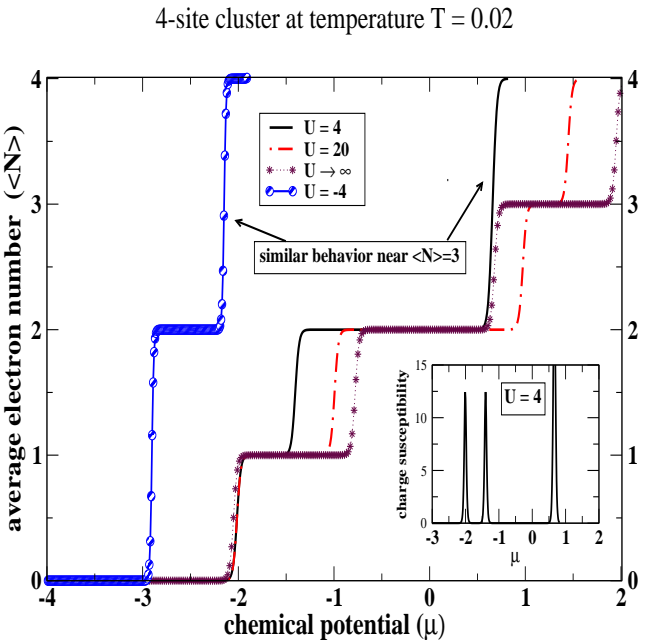


FIG. 1: Variation of average electron concentration versus  $\mu$  in ensemble of 4-site clusters for various  $U$  values. The result for  $U = -4$  is given for comparison with  $U = 4$ . The inset shows the variation of charge susceptibility  $\chi_c$  versus  $\mu$  for  $U = 4$ .

or quadruplet) coupling. Using the above definitions for  $h_{\pm}$  we can combine both as,

$$\Delta^s(T) = \begin{cases} \Delta^{AF}(T), & \text{for } h_+ > h_- \\ \Delta^F(T) & \text{for } h_- > h_+ \end{cases} \quad (7)$$

This natural order parameter in a multidimensional parameter space  $\mu, U, T$  at nonzero temperature will be called a *spin pairing pseudogap*. We define the crossover temperatures  $T_s^P$  and  $T_F$  as the temperatures at which the corresponding spin pseudogaps vanish and a spin paramagnetic state, with  $h_- = h_+$ , is stable. Similarly, following the peaks in *zero magnetic field* spin susceptibility, a spin pseudogap  $\Delta^s(T)$ , and an associated  $T_s(\mu)$  can be defined [23].

## IV. RESULTS

### A. $\langle N \rangle$ versus $\mu$

In Fig. 1 for the 4-site cluster, we explicitly show the variation of  $\langle N \rangle$  versus  $\mu$  below half filling for various  $U$  values in order to track the variation of charge gaps with  $U$ . The opening of the gap is a local correlation effect, and clearly does not follow from long range order, as exemplified here. For infinitesimal  $U > 0$ , true gaps at  $\langle N \rangle = 1, 2$  develop and they increase monotonically with  $U$ . In contrast, the charge gap at  $\langle N \rangle = 3$  opens at

$U \geq U_c(0)$  (a critical value; see Ref. [23]) and relatively low temperatures. Thus at low temperature,  $\langle N \rangle$  (expressed as a function of  $\mu$  in Fig. 1) evolves smoothly for  $U \leq U_c(0)$ , and shows finite leaps across the MH plateaus at  $\langle N \rangle = 2, 4$ . In Fig. 1, in the vicinity  $\langle N \rangle = 3$ , one can notice two phases. At  $U \leq U_c(T)$ , a negative charge gap with midgap states is a signature of electron-electron pairing at low temperatures. For  $U \geq U_c(T)$ , the MH-like charge gap in (5) is positive  $\mu_+ > \mu_-$ , which favors electron-hole pairing similar to MH gap at half filling. As  $U$  increases,  $\langle s^z \rangle$  versus  $\mu$  reveals islands of stability; the minimal spin state  $\langle s^z \rangle = 0$  at  $U \leq U_c(0)$ ; unsaturated ferromagnetism  $\langle s^z \rangle = \frac{1}{2}$  at  $U_c(0) < U < U_F(0)$ ; saturated Nagaoka ferromagnetism, with maximum spin  $\langle s^z \rangle = \frac{3}{2}$  at  $U > U_F(0)$  (not shown in Fig. 1). As  $U \rightarrow \infty$ , the charge and spin gaps at  $\langle N \rangle \simeq 3$  gradually saturate to its maximum  $\rightarrow 2(2 - \sqrt{2})t$  and  $2 - \sqrt{3}$  values respectively. At  $\langle N \rangle \simeq 2$ , we have full charge-spin reconciliation when the spin gap at quarter filling approaches the charge gap,  $4(\sqrt{2} - 1)t$ , as  $U \rightarrow \infty$ . The chemical potential gets pinned upon doping in the midgap states at  $\langle N \rangle \simeq 3$  and  $U = 4$ . Such a density profile of  $\langle N \rangle$  versus  $\mu$  near  $\langle N \rangle = 3$ , closely resembles the one calculated at  $U = -4$  for the attractive 4-site Hubbard cluster in Fig. 1 and, is indicative of possible particle or hole pairing.

### B. Quantum critical points

The exact expression for the charge gap,  $\Delta_3^c(U : 0)$ , at  $\langle N \rangle \simeq 3$  has been derived earlier in Ref. [22]. At zero temperature, the sharp transition at critical parameter  $U_c(0)$  is defined from the condition  $\Delta_3^c(U_c : 0) \equiv 0$  which yields,  $U_c(0) = 4.58399938$ . The vanishing gap at  $U_c(0)$  in the ground state can be directly linked to the quantum critical point [31] (QCP) for the *onset of pair formation*. Indeed the QCP,  $U = U_c(0)$ , separates electron-electron pairing from MH-like electron-hole pairing regime. The QCP turns out to be a useful point for the analysis of the phase diagram at zero and non-zero temperatures. The QCP and the corresponding singular doping dependencies on the chemical potential and the departure from that point at nonzero crossover temperatures on  $T - \mu$  phase diagrams for various  $U$  values are given in section IV F. Exactly at  $U = U_c(0)$  there is no charge-spin separation and, a spin paramagnetic state coexists with a Fermi liquid similar to non-interacting electrons, where  $U = 0$ . At zero temperature the analytical expression for the charge gap first was derived in Ref. [22]. Using definition introduced in (5), the corresponding electron-electron pairing gap,  $\Delta^P(0)$ ,

$$\Delta^P(0) = -\frac{2}{\sqrt{3}}\sqrt{(16 + U^2)} \cos \frac{\gamma}{3} - \frac{U}{3} + \frac{2}{3}\sqrt{(48 + U^2)} \cos \frac{\alpha}{3} - \sqrt{32 + U^2 + 4\sqrt{64 + 3U^2}}, \quad (8)$$

exists only at  $U < U_c(0)$ . In contrast, the electron-hole pairing is zero at  $U < U_c(0)$  and exists in the ground

state only for all  $U > U_c(0)$ . The electron-hole pairing gap,  $\Delta^{e-h}(0)$ , within the range  $U_c < U < U_F(0)$  is

$$\Delta^{e-h}(0) = \frac{2}{\sqrt{3}} \sqrt{(16+U^2)} \cos \frac{\gamma}{3} + \frac{U}{3} + \sqrt{32+U^2+4\sqrt{64+3U^2}} - \frac{2}{3} \sqrt{(48+U^2)} \cos \frac{\alpha}{3}, \quad (9)$$

Above the critical point  $U \geq U_F(0)$  the electron-hole gap is

$$\Delta^{e-h}(0) = \frac{2}{\sqrt{3}} \sqrt{(16+U^2)} \cos \frac{\gamma}{3} - \frac{2}{3} \sqrt{(48+U^2)} \cos \frac{\alpha}{3} + \frac{U}{3} + 4. \quad (10)$$

where corresponding parameters in Eqs. (8), (9) and (10)  $\alpha = \arccos\{(\frac{4U}{3} - \frac{U^3}{27})/(\frac{16}{3} + \frac{U^2}{9})^{\frac{3}{2}}\}$  and  $\gamma = \arccos\{(4U)/(\frac{16}{3} + \frac{U^2}{3})^{\frac{3}{2}}\}$ . At relatively large  $U \geq 4.584$ , the energy gap  $\Delta_3^c(U : 0)$  becomes positive for  $\langle N \rangle = 3$ . With increasing temperature, this pseudogap  $\Delta_3^c(U : T)$  increases. Due to (ground state) level crossings, the spin degeneracy in an infinitesimal magnetic field is lifted at QCP,  $U_F(0) = 8 + 4\sqrt{7} \simeq 18.583$  (10) and the ground state becomes a ferromagnetic insulator with the maximum spin  $\langle s^z \rangle = \frac{3}{2}$  [23, 32]. The critical value,  $U_c(T)$  at which  $\Delta_3^c(U : T) = 0$ , depends on the temperature. At  $U < U_c(0)$ ,  $\Delta_3^c(T)$  in a limited range of  $U$  is negative [23]. Thus according to Eq. (2), the states with  $\langle N \rangle = 3$  become energetically less favorable when compared with  $\langle N \rangle = 2$  and  $\langle N \rangle = 4$  states. This is explicit evidence for the electron phase separation instability and the existence (at finite temperature) of particle-particle or hole-hole binding despite a bare electron repulsion. At zero temperature,  $U > U_F(0)$  and  $\langle N \rangle = 3$ , the calculated spin gap  $\Delta_3^s(U : T)$ , for transition from  $\langle s^z \rangle = \frac{1}{2}$  to  $\langle s^z \rangle = \frac{3}{2}$ ,

$$\Delta_3^s(U : T = 0) = \frac{\sqrt{32+U^2+4\sqrt{64+3U^2}}}{2} - 2 - \frac{U}{3} \quad (11)$$

is also negative, which manifests a thermodynamic instability ( $\chi_s < 0$ ) and the phase separation into ferromagnetic "domains" with  $\langle s^z \rangle = \frac{3}{2}$  and  $\langle s^z \rangle = -\frac{3}{2}$  in the ensemble of clusters. Thus we can classify and see various phases, phase transitions and phase separations in finite systems. Therefore, phase transitions in interacting many-body system is not a characteristic of an infinitely large thermodynamic system, but can well be defined in canonical and grand canonical ensembles for finite systems without the use of the thermodynamic limit.

### C. Electron charge and spin pairings

The fact that electron pairing can arise directly from the on-site electron repulsion between electrons in small clusters was found quite early [33, 34, 35, 36]. However,

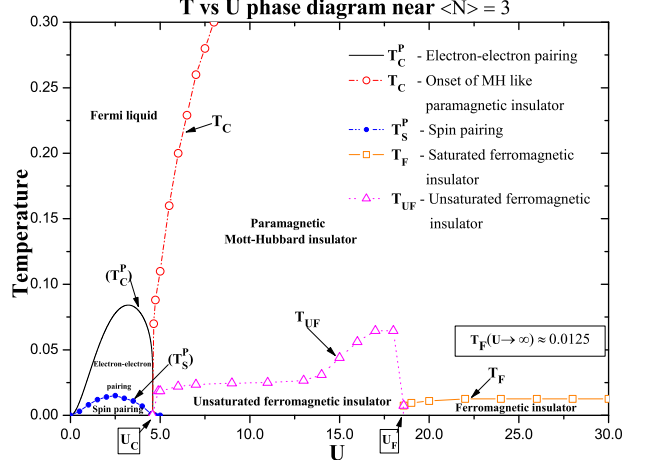


FIG. 2: Crossover temperatures versus  $U$  for 4-site phase diagram near optimally doped  $\langle N \rangle = 3$  regime. Here  $T_c$  denotes the crossover temperature for the onset of the MH-like paramagnetic insulator with electron-hole pairing gap and spin (gapless) liquid, onset of electron-electron pairing below  $T^P$ , Bose condensation of electron charge and coupled spin pairs below  $T_s^P$ , unsaturated ( $T_{UF}$ ) and saturated ferromagnetic ( $T_F$ ) crossovers in MH-like insulators with electron-hole pairing. Note that electron-electron pairing is unlikely to occur above  $T > 0.08$  in a spin (gapless) liquid phase. The energies and temperatures are measured in units of  $t = 1$ , the hopping parameter.

it is not *a priori* obvious that such a mechanism in an ensemble of small clusters can survive at finite temperatures. Our exact solution demonstrates that it does survive. In Fig. 2, we show condensation with bound, double electron charge and decoupled spin at  $U \leq U_c(0)$  and  $T_s^P(U) \leq T \leq T_c^P(U)$ . Below  $T_s^P(U)$ , the spin degrees are also condensed with 'bosonization' of spin and charge degrees and possible 'superconductivity'. As an important observation we found is that the variation of pairing gaps,  $\Delta^P(U)$  and  $\Delta^{e-h}(U)$  versus  $U$ , in the ground state closely follows the variation of  $T_c^P(U)$ , and  $T_c(U)$  respectively. For  $U \leq U_c(0)$  there is correlation between the spin pairing gap  $\Delta_s^P(U)$  and corresponding crossover temperature  $T_s^P(U)$  versus  $U$ . At larger  $U \geq U_c(0)$ , we found similar correlations in  $U$  space between ferromagnetic spin pairing gaps and corresponding ferromagnetic crossover temperatures.

Our calculations for the  $U \leq U_c$  range may also be used to reproduce the behavior of  $T_c(p)$  versus pressure  $p$  in the HTSCs, if we assume that the parameter  $U$  decreases with increasing pressure. In Fig. 2, the crossover temperatures for electron-electron,  $T_c^P$ , electron-hole,  $T_c$ , and, coupled spin,  $T_s^P$ , pairings are plotted as a function of  $U$ . The shown condensation of both doubled electron charge, and zero spin  $s^z = 0$  (singlet) degrees below  $T_s^P$  is indicative of a possible mechanism of superconductivity in the HTSCs near optimal doping. In the HTSCs, superconducting transition temperature  $T_c$  generally in-

creases with pressure first, reaches the maximum value at some critical pressure  $p_c$  and then decreases with pressure [39] in agreement with our result for the variation of  $T_s^P(U)$  versus  $U$ . These pressure effects in the cuprate family reflect the changes in electron pairing due to the moderate Coulomb interaction  $U$ . Notice, that at enough large  $U$ ,  $T_c(p)$  decreases with  $U$  under pressure, as it is shown in Fig. 2. This might explain why the pressure  $T_c(p)$  decreases across some of organic and families alkali doped fullerene superconductors [40].

Our results for  $N \approx 3$  in Fig. 2 suggest that the enhancement of  $T_c$  in the parental MH cuprates, with relatively large  $U$  in the optimally doped HTSCs, can be due to an increase of pairing by decreasing  $U$  under pressure rather than an increase of the pressure-induced hole concentration. Thus it appears that the 4-site cluster near  $N \approx 3$  indeed captures the essential physics of the pressure effect on electron pairing and BC in HTSCs near optimal doping. Similarly, our calculations in Fig. 2 for  $U \geq U_c$  range can also be useful in predicting the variation of  $T_{UF}(p)$  and  $T_F(p)$  versus pressure  $p$  in ferromagnetic insulators and Co-doped anatase  $\text{TiO}_2$  [11].

#### D. Charge-spin separation

Until recently, electrons were thought to carry their charge and spin degrees simultaneously. It is certainly true for non-interacting electrons, where  $U = 0$ . At zero temperature, a paramagnetic Fermi liquid with zero charge and spin gaps in Fig. 2 exists only at  $U = 0$  and  $U = U_c(0)$ . At finite temperatures the corresponding charge pseudogaps vanish at particle-particle/hole pairing crossover temperatures and there is also no sign of charge and spin separation above  $T_c$  and  $T_c^P$ . However, as temperature decreases below these crossover temperatures only the charge pseudogaps are formed, while spin excitations remain gapless and these paramagnetic spin liquid states coexisting with electron-electron or MH-like electron-hole pairings will be labeled as a charge-spin separation. Gapless spin response due to small variations of magnetic field or electron concentration (chemical potential) is independent of the charge degrees of freedom. By decreasing temperature, a partial charge-spin reconciliation takes place in Fig. 2 below ferromagnetic crossover temperatures due to the formed spin pseudogap with coupled charge and spin degrees. Accordingly, electron-hole pairs and ferromagnetic coupled spins are bounded in charge and spin sectors below ferromagnetic crossover temperature. The effect of charge-spin separation becomes stronger with increasing  $U > U_c(0)$ , since the distinction between the corresponding charge and spin crossover temperatures increases with  $U$  (see Fig. 2).

In Fig. 3, we examine the behavior of charge and spin degrees of freedom below the spin condensation temperature  $T_s^P$ . Fig. 3 shows how the spin degrees, at an infinitesimal magnetic field, follow the charge. Notice how strong inter-configuration charge and spin fluctua-

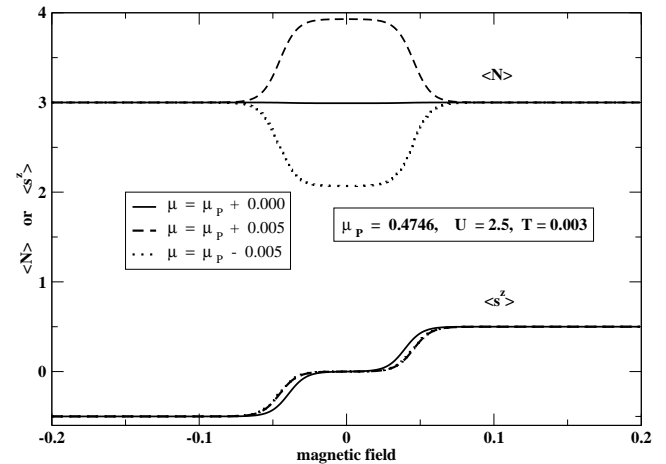


FIG. 3: The average number of electrons and magnetization dependencies versus an applied magnetic field at  $U = 2.5$ ,  $T = 0.003$  and  $\mu_p = 0.4746$ . Note how a small change in the chemical potential (from  $\mu_p \pm 0.005$ ) forces the (paired) system into a magnetic spin liquid state with an unpaired spin and  $N \approx 3$ .

tions can be monitored by small variation of a chemical potential or magnetic field. The coupling between the spin and charge degrees of freedom is manifested due to the composite nature of the electron, having charge (holon) and spin (spinon). Thus, the spin singlet pairing in the spin sector and the electron-electron or hole-hole pairings in the charge sector are not independent but demonstrate coherency and a strong coupling between them, which is necessary for possible 'superconductivity'. Below the critical temperature of crossover  $T_c^P$ , the charge degrees are coupled and simultaneous condensation of spin degrees below  $T_s^P$  results in reconciliation of charge and spin and possible full 'bosonization' of electrons. Thus the electron fragments into the charge and spin excitation states and superconductivity arises due to the charge-spin separation and subsequent condensation of these charge and spin degrees that are both bosonic in nature [5].

#### E. Phase separation

The mechanism of phase separation (i.e segregation) in small clusters near  $\langle N \rangle = 3$  is also quite straightforward and simply depends on the pairing conditions in charge and spin channels respectively [23]. At  $U > U_c(0)$  in Fig. 2, we notice a stable ferromagnetic state with unsaturated magnetization and a ferromagnetic state with saturated Nagaoka magnetization at larger  $U > U_F(0)$  values. As temperature increases the system undergoes a smooth crossover from a ferromagnetic MH-like insulator with  $\Delta^{e-h} \neq 0$  and  $\Delta_F \neq 0$  into a paramagnetic MH insulator with  $\langle s^z \rangle \approx 0$ . The ferromagnetic critical temperature  $T_F(U)$  increases monotonically with  $U$  and

as  $U \rightarrow \infty$  the limiting  $T_F(U \rightarrow \infty) = 0.0125$  value approaches to the maximum spin pairing temperature  $T_s^P$ . A ferromagnetic phase with broken symmetry was obtained here in the presence of an infinitesimal magnetic field and increasing temperature leads to a F-PM transition and restoration of the symmetry in paramagnetic phase. The level crossing at  $U_c(0)$  ( $U_F(0)$ ) in the presence of an appropriate infinitesimal magnetic field brings about phase separation of the thermodynamically unstable ensemble of clusters with  $h_- > h_+$  into spin up and spin down ferromagnetic "domains" (see section IV A).

It appears that the canonical approach yields also an adequate estimation of possible pair binding instability near  $\langle N \rangle = 3$  in an ensemble of small clusters at relatively low temperature and moderate  $U \leq U_c(0)$ . New important features appear if the number of electrons  $\langle N \rangle = 3$  is kept fixed for the whole system of decoupled clusters, placed in the (particle) bath, by allowing the particle number on each separate cluster to fluctuate. One is tempted to think that due to symmetry, there is a single hole on each cluster within the  $\langle N \rangle = 3$  set in the ensemble. However, due to thermal and quantum fluctuations in the density of holes between the clusters  $U < U_c(0)$ , it is energetically more favorable to form pairs of holes. In this case, snapshots of the system at relatively low temperatures and at a critical value ( $\mu_P$  in Fig. 4) of the chemical potential would reveal equal probabilities of finding (only) clusters that are either hole rich ( $\langle N \rangle = 2$ ) or hole poor ( $\langle N \rangle = 4$ ). Thus ensemble of 4-site clusters at  $\langle N \rangle = 3$  is thermodynamically unstable,  $\mu_+ \leq \mu_-$ , and can lead to macroscopic phase separation onto hole-rich and hole-poor regions recently detected in super-oxygenated  $\text{La}_{2-x}\text{Sr}_x\text{CuO}_{4+y}$ , with various Sr contents [10, 23].

The level crossing under slight doping (infinitesimal variation of chemical potential) brings about phase separation of ensemble of clusters and this can be linked to the formation of inhomogeneity, consisting of hole-poor (superconducting) and hole-rich (antiferromagnetic) "domains" at  $U < U_c(0)$ . Thus we can conclude that ensemble of 4-site clusters with  $\langle N \rangle = 3$  at relatively low temperatures is unstable for all  $U > 0$  values with regard to phase separation due to spontaneous symmetry breaking into ferromagnetic or superconducting "domains" either in spin or charge sectors respectively.

The  $T$ - $\mu$  phase diagram for the 4-site cluster near  $\mu_P$ , is shown in Fig. 4. This exact phase diagram at  $U = 4$  in the vicinity of the optimally doped ( $N \approx 3$ ) regime has been constructed based on the condition  $\Delta^c(T) < 0$  with  $\mu_-(T) > \mu_+(T)$ , reported earlier in Ref. [23]. The electron pairing temperature,  $T_c^P$ , identifies the onset of charge pairing. As temperature is further lowered, spin pairs begin to form at  $T_s^P$ . At this temperature (with zero magnetic field), spin susceptibilities become very weak indicating the disappearance of the  $\langle N \rangle \approx 3$  states. Below this spin pairing temperature, only paired states in "metallic" liquid ( $\Delta^{e-h} = 0$ ) in the midgap region are observed to exist having a certain rigidity, so that

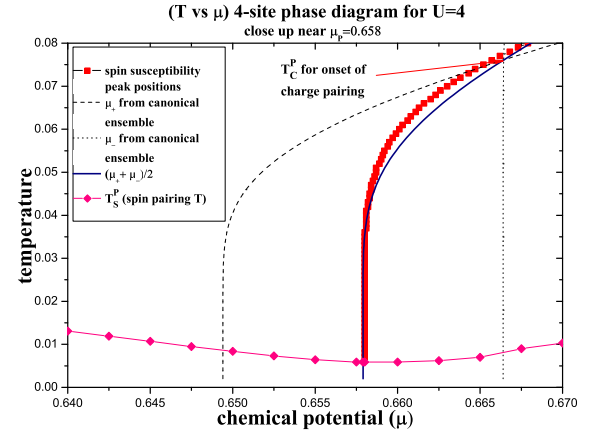


FIG. 4: The phase  $T$ - $\mu$  diagram in canonical ensemble of four-site clusters close to  $\langle N \rangle \approx 3$  and  $\mu_P = 0.658$  at  $U = 4$ . The phase below  $T_c^P$  suggests the existence of electron-electron pairing at finite temperature with unpaired spin states. The zero (magnetic) spin susceptibility peak in spin (melted) liquid state terminates at finite  $T_s^P$  and as temperature is further lowered the spin pairs begin to form. This picture with  $\mu_-(T) > \mu_+(T)$  supports the idea that there is inhomogeneous, electronic phase separation here. As  $U$  increases above  $U_c(0) = 4.584$ , these inhomogeneities disappear and a stable unsaturated ferromagnetic MH-like insulating region emerges around optimal doping shown in Fig. 5.

a nonzero magnetic field or a finite temperature is required to break the pairs. From a detailed analysis, it becomes evident that the system is on the verge of an instability; the paired phase competing with a phase that suppresses pairing which has a high, zero-field magnetic susceptibility. As the temperature is lowered, the number of  $\langle N \rangle \approx 3$  (unpaired) clusters begins to decrease while a mixture of (paired)  $\langle N \rangle \approx 2$  and  $\langle N \rangle \approx 4$  clusters appears. In Fig. 4 the spin pairing phase below  $T_s^P$  competes with a phase (having a high magnetic susceptibility) that suppresses pairing at 'moderate' temperatures. Surprisingly, the critical doping  $\mu_P$  (which corresponds to a filling factor of 1/8 hole-doping away from half filling), where the above pairing fluctuations take place when  $U < U_c(0)$ , is close to the doping level near which numerous intriguing properties have been observed in the hole-doped HTSCs. For example, the spin pseudogap can be driven to zero also by applying a suitable magnetic field. This factor leads to the stability of electron "dormant" magnetic configuration in a narrow, critical doping region close to  $\langle N \rangle \approx 3$ , competing with  $\langle N \rangle = 2$  and  $\langle N \rangle = 4$  states as have seen in a recent experiment [10]. Thus our results, at electron concentration  $\langle N \rangle \approx 3$ , clearly demonstrate phase separation and breakdown of Fermi liquid behavior due to electron-electron/hole pairings and Nagaoka ferromagnetism in the absence of long-range order.

### F. Phase diagrams

In Figs. 4 and 5, the phase diagrams for the ensemble of 4-site clusters are shown, where we define the charge peak (i.e maxima)  $T_c(\mu)$  to be the temperature with maximum  $\chi_c(\mu)$  at a given  $\mu$ . Possible peaks in the zero magnetic field spin susceptibility  $\chi_s(\mu)$ , when monitored as a function of  $\mu$ , can also be used to define an associated temperature,  $T_s(\mu)$ . In addition, for a given  $\mu$ ,  $T_{AF}(\mu)$  defines the temperature at which AF (spin) gap disappears, i.e.  $\Delta^s(T_{AF}) = 0$ . These have been constructed almost exclusively using the temperatures,  $T_c(\mu)$ ,  $T_s(\mu)$  and  $T_{AF}(\mu)$ , defined previously. We have identified the following phases in these diagrams: (I) and (II) are charge pseudogap phases separated by a phase boundary where the spin susceptibility reaches a maximum, with  $\Delta^{e-h}(T) > 0$ ,  $\Delta^{AF}(T) = 0$ ; at finite temperature, phase I has a higher  $\langle N \rangle$  and coupled spin compared to phase II spin liquid phase; Phase (III) is a MH-like antiferromagnetic insulator with bound charge and spin, when  $\Delta^{e-h}(T) > 0$ ,  $\Delta^{AF}(T) > 0$ ; phase separation (PS) in  $T - \mu$  plane for  $U = 4$  with a vanished charge gap at  $\langle N \rangle = 3$ , now corresponding to the opening of a pairing gap ( $\Delta^P(T) > 0$ ) in the electron-electron channel with  $\Delta_3^c(U : T) < 0$ . We have also verified the well known fact that the low temperature behavior in the vicinity of half filling, with charge and spin pseudogap phases coexisting, represents an AF insulator [22]. However, away from half filling, we find very intriguing behavior in thermodynamical charge and spin degrees of freedom. In both phase diagrams, we find similar MH-like (I), (II) and AF-like (III) charge-spin separated phases in the hole-doped regime. In Fig. 5, spin-charge separation in phases (I) and (II) originates for relatively large  $U$  in the underdoped regime. In contrast, Fig. 4 shows the existence (at  $U = 3$ ) of a line phase (with pairing) similar to  $U < 0$  case with electron pairing ( $\Delta^P(T) > 0$ ), when the chemical potential is pinned up on doping within the highly degenerate midgap states near (underdoped) 1/8 filling.

Among other interesting results, rich in variety for  $U > 0$ , sharp transitions and quantum critical points (QCPs) are found between phases with true charge and spin gaps in the ground state; for infinitesimal  $T > 0$ , these gaps are transformed into ‘pseudogaps’ with some nonzero weight between peaks (or maxima) in susceptibilities monitored as a function of doping (i.e.  $\mu$ ) as well as  $h$ . We have also verified the well known fact that the low temperature behavior in the vicinity of half filling, with charge and spin pseudogap phases coexisting, represents an AF insulator in the Hubbard clusters [22]. However, away from half filling, we find very intriguing behavior in thermodynamical charge and spin degrees of freedom. In both phase diagrams, we find similar MH-like (I), (II) and AF-like (III) charge-spin separated phases in the hole-doped regime. In Fig. 5, spin-charge separation in phases (I) and (II) originates for relatively large  $U$  in the underdoped regime. We have also seen that a reasonably strong magnetic field has a dramatic effect

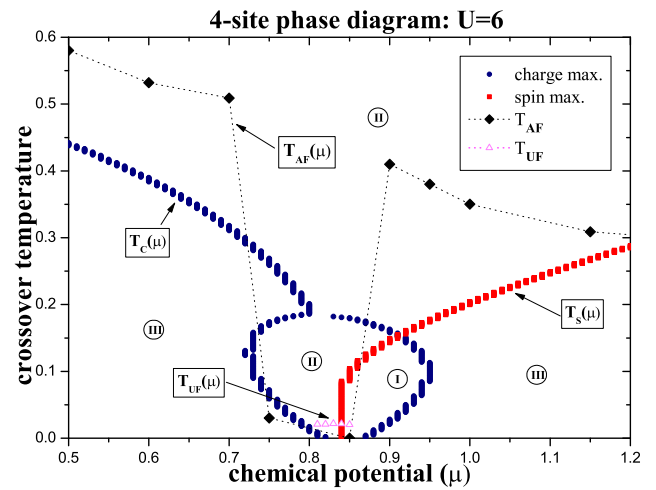


FIG. 5: Temperature  $T$  vs chemical potential  $\mu$  phase diagram for the grand canonical ensemble of four-site clusters at  $U = 6$  and  $h = 0$ . Regions I, II and III are quite similar to the ones found in enlarged Fig. 4 for  $U = 4$  [23], again showing strong charge-spin separation. However, a charge gap opens as a new bifurcation (I and II phases) which consists of charge and spin pseudogaps, (replacing the line phase P in the previous figure: see text). In the vicinity of  $\langle N \rangle \approx 3$  below  $T_{UF}(\mu)$  unsaturated ferromagnetism coexists with the MH-like insulator.

(mainly) on the QCP at  $\mu_s$ , at which the spin pseudogap disappears. The regions (I) and (II), with the prevailing charge gap  $\Delta^c(T) > 0$ , are separated by a boundary where the spin gap vanishes. At critical doping  $\mu_s$  with  $T_s \rightarrow 0$ , the zero spin susceptibility  $\chi_s$  exhibits a sharp maximum. The critical temperature  $T_s(\mu)$ , which falls abruptly to zero at critical doping  $\mu_s$ , implies [15] that the pseudogap can exist independently of possible superconducting pairing in Fig. 5. In contrast, Fig. 4 shows the existence at  $U = 3$  of a line phase (with pairing) similar to  $U < 0$  case with a spin pseudogap ( $\Delta^s(T) > 0$ ) and electron pairing pseudogap ( $\Delta^P(T) > 0$ ), when the chemical potential is pinned up on doping within the highly degenerate midgap states near (underdoped) 1/8 filling.

We have also seen that a reasonably strong magnetic field has a dramatic effect (mainly) on the QCP at  $\mu_s$ , at which the spin pseudogap disappears. It is evident from our exact results that the presence of QCP at zero temperature and critical crossover temperatures, give strong support for cooperative character of existing phase transitions and crossovers in finite size clusters as in large thermodynamic systems [37, 38].

As an important remark, in the noninteracting case,  $U = 0$ , the charge and spin peaks follow one another (in sharp contrast to the  $U = 4$  and 6 cases, in regions I and II where charge (as well as spin) maxima and minima are well separated) indicating that there is no charge-spin separation, even in the presence of a magnetic field. In the entire range of  $\mu$ , the charge and spin fluctuations

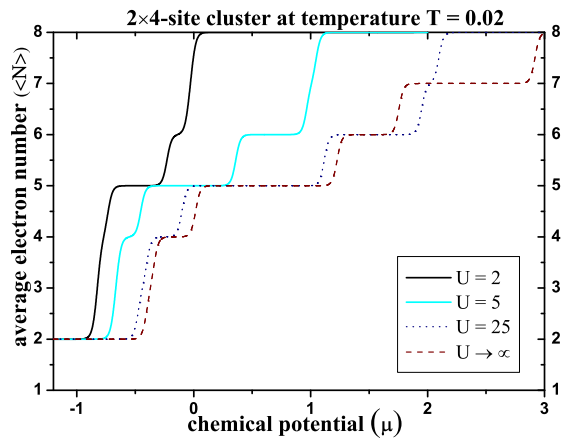


FIG. 6: Variation of average electron concentration versus  $\mu$  in ensemble of  $2 \times 4$  clusters with the couplings  $c = 1$  between the squares for various  $U$  values,  $h = 0$  and  $T = 0.02$ . Here we can easily identify regions quite similar to the ones found in Fig. 1, showing strong charge-spin separation with various crossover temperatures. This phase suggests the existence of electron-electron pairing at low temperatures,  $T \leq 0.028$ .

directly follow one another, i.e. without charge-spin separation. For interacting electrons, we notice similar respond of charge and spin degrees at  $\langle N \rangle = 3$  only at single point,  $U = U_c(0)$ . In the atomic limit,  $t = 0$ , a full charge-spin separation, exactly at half filling, takes place in the ground state and the corresponding MH crossover temperature of the metal-insulator transition occurs at  $T_{MH} = U/(2 \ln 2)$ .

### G. Coupled 4-site clusters

We have also carried out exact numerical diagonalization and calculations of the charge gap and pairing in 8-site,  $2 \times 4$  planar clusters with periodic boundary conditions in both directions, to illustrate similar effects on the properties described above for the 4-site clusters. The pairing fluctuations that are seen for the 4-site cluster are found to exist for  $2 \times 4$  ladders near half filling ( $\langle N \rangle \approx 7$ ) as well. Most of the trends observed for the 4-site clusters, such as the MH-like charge (pseudo) gap, AF-like (pseudo) gap, (spin) pseudogap, electron and spin pairing (pseudo) gaps and with corresponding crossover temperatures are also observed here. Moreover, we find corresponding critical  $U_c(0)$  and  $U_F(0)$  values for the pairing instabilities and vanishing of corresponding pseudogaps at finite temperatures  $T_{UF}$  and  $T_F$  similar to the 4-site cluster. The fluctuations that occur here at optimal doping are among the states with  $\langle N \rangle \approx 6, 7$  and 8 electrons. At  $\langle N \rangle \approx 7$ , we clearly observe the dormant magnetic state as noticed in the 4-site cluster with a slight variation of the chemical potential or magnetic field. Thus our

exact cluster simulations of the Hubbard model displays incipient pairing, ferromagnetism, phase separation and other phenomena are remarkably similar to those found in small nanoparticles, transition metal oxides and high  $T_c$  cuprates [14].

## V. CONCLUSION

In summary, we have illustrated how to obtain phase diagrams and identify the presence of temperature driven particle-particle/hole and spin pairing crossovers below  $U < U_c(0)$ , quantum critical points ( $\mu_s, \mu_c$ ) and charge-spin separation regions for any  $U > U_c(0)$  in the ensemble of 4-site Hubbard *clusters* as doping (or chemical potential) is varied. Specifically, our exact solution pointed out an important difference between the  $U = 4$  and  $U = 6$  phase diagrams near half filling (i.e. one hole off half filling), which can be tied to electron-electron pairing and possible superconductivity and ferromagnetism in doped HTSCs and transition metal oxides or disulfides respectively. Our results show the pairing crossover near  $\langle N \rangle \approx 3$  and strongly suggest that particle-particle pairing and spin coupling can exist at  $U < U_c(0)$ , while particle-hole binding and ferromagnetism is presumed to occur for  $U > U_c(0)$ . Exactly at  $U = U_c$ , paramagnetic Fermi liquid is stable in the ground state and all finite temperatures. At  $U > U_F(0)$ , there is another subsequent transition into a saturated ferromagnetic insulator with maximum spin  $\langle s^z \rangle \approx \frac{3}{2}$ . It is also apparent that short-range correlations alone are sufficient for pseudogaps to form in small 4-site and larger  $2 \times 4$  clusters, which can be linked to the generic features of phase diagrams in temperature and doping effects seen in the HTSCs. The exact cluster solution shows how charge and spin gaps are formed at the microscopic level and their behavior as a function of doping (i.e. chemical potential), magnetic field and temperature. The spin and charge crossover temperatures can also be associated with the formation of pairing gaps below  $T_c^P(U)$ . As temperature decreases further, a simultaneous BC of spin degrees of freedom takes place below  $T_s^P(U)$ . The increase of  $T_s^P(U)$  with decrease of  $U$  below  $U_c$  in Fig. 2 reproduces the variation of  $T_c$  versus  $p$  in the optimally and nearly optimally doped HTSC materials [39], which suggests a significant increase of pairing temperature  $T_c$  under pressure or  $U$  due to the enhancement of the zero temperature charge and spin pairing gaps. In addition, our calculations provide important benchmarks for comparison with Monte Carlo, RSRG, PCT and other approximations.

Finally, we have developed novel theoretical concepts and techniques, which are especially suitable and efficient for understanding of nascent superconductivity and magnetism using the canonical and grand canonical ensemble for small clusters. Our results show the cooperative *nature* of phase transition phenomena in finite-size clusters similar to large thermodynamic systems. The developed approach allows an exact and unbiased study

of the Fermi liquid instabilities in small clusters without the assumption of a broken symmetry. The small *nanoclusters* exhibit particle-particle, spin-spin pairings in a limited range of  $U$ ,  $\mu$  and  $T$  and share very important intrinsic characteristics with the HTSCs and magnetic oxides. These ideas could be useful in different areas outside the cluster field, to systems ranging from molecules

to continuous media, and applied for understanding of phase separation and incipient spontaneous superconductivity and ferromagnetism in small nanometer-scale clusters and Nb, Co nanoparticles [1, 2, 3, 4]. This research was supported in part by the U.S. Department of Energy under Contract No. DE-AC02-98CH10886.

---

[1] Xiaoshan Xu, Shuangye Yin, Ramiro Moro, and Walt A. de Heer, Phys. Rev. Lett. **93**, 086803 (2004).

[2] X. Xu, S. Yin, R. Moro, and W. A. de Heer, Phys. Rev. Lett. **95**, 237209 (2005); R. Moro, S. Yin, X. Xu, and W. A. de Heer, Phys. Rev. Lett. **93**, 086803-1 (2004).

[3] C. T. Black, D. C. Ralph and M. Tinkham, Phys. Rev. Lett. **78**, 4087 (1997).

[4] A. J. Cox, J. G. Louderback, S. E. Apsel, and L. A. Bloomfield Phys. Rev. B**49**, 12295 (1994).

[5] P. W. Anderson, Adv. Phys. **46**, 3 (1997); Science **235**, 1196 (1987).

[6] V. Emery and S. A. Kivelson, Nature (London), **374**, 434 (1995).

[7] T. Timusk and B. Statt, Rep. Prog. Phys. **62**, 61 (1999).

[8] S. A. Kivelson *et al.*, Rev. Mod. Phys. **75**, 1201 (2003).

[9] D. S. Marshall *et al.*, Phys. Rev. Lett.

[10] H. E. Mohottala *et al.*, Nature Mater. **5**, 377 (2006).

[11] Y. Matsumoto, M. Murakami, T. Shono, T. Hasegawa, T. Fukumura, M. Kawasaki, P. Ahmet, T. Chikyow, S. Koshihara, and H. Koinuma, Science **291**, 854 (2001).

[12] Y. Nagaoka, Phys. Rev. B**147**, 392 (1966).

[13] J. B. Sokoloff, Phys. Rev. B**2**, 37073713 (1970).

[14] E. L. Nagaev, Phys. Uspekhi **39**, 781 (1996).

[15] G. V. M. Williams, J. L. Tallon and J. W. Loram, Phys. Rev. B**58**, 15053 (1998).

[16] A. Damascelli, Z. Hussain, Z.-X. Shen, Rev. Mod. Phys. **75**, 473 (2003).

[17] V. J. Emery, S. A. Kivelson and O. Zachar, Phys. Rev. B**56** 6120 (1997).

[18] J.S. Schilling and S. Klotz, in Physical Properties of High Temperature Superconductors (edited by D.M. Ginzberg), Vol.3 pp. 59-157 (World Scientific, Singapore, 1992).

[19] Y. Zha, V. Barzykin and D. Pines, Phys. Rev. B**54**, 7561 (1996).

[20] H. Shiba and P. A. Pincus, Phys. Rev. B**5**, 1966 (1972).

[21] R. Schumann, Ann. Phys. **11**, 49 (2002).

[22] A. N. Kocharian, G. W. Fernando, K. Palandage and J. W. Davenport, J. Magn. Magn. Mater. **300**, 585 (2006).

[23] A. N. Kocharian, G. W. Fernando, K. Palandage and J. W. Davenport, Phys. Rev. B**74**, 24511-1 (2006).

[24] D. Sénéchal, D. Perez, and M. Pioro-Ladrière, Phys. Rev. Lett. **84**, 522 (2000).

[25] W.-F. Tsai and S. A. Kivelson, Phys. Rev. B**73**, 214510 (2006); APS March Meeting Bulletin **51** (1), Part 2 (2006).

[26] J. Malrieu and N. Guihery, Phys. Rev. B**63**, 085110 (2001).

[27] E. Altman and A. Auerbach, Phys. Rev. B**65**, 104508 (2002).

[28] M. Jarrell, Th. Maier, M.H. Hettler, and A.N. Tahvildarzadeh, Europhys. Lett. **56**, 563 (2001).

[29] A. N. Kocharian and Joel H. Sebold, Phys. Rev. B**53**, 12804 (1996).

[30] E. H. Lieb and F. Y. Wu, Phys. Rev. Lett. **20**, 1445 (1968).

[31] S. Sachdev, Quantum Phase Transitions, Cambridge University Press, Cambridge U.K. (1999).

[32] D. C. Mattis, Int. J. Nanoscience **2**, 165 (2003).

[33] N. E. Bickers, D. J Scalapino, and R. T. Scalettar, Int. J. Mod. Phys. B**1** 687 (1987).

[34] R. M. Fye, M. J. Martins, and R. T. Scalettar, Phys. Rev. B**42**, R6809 (1990).

[35] S. R. White, S. Chakravaarty, M. P. Gelfand, and S. A. Kivelson, Phys. Rev. Lett. **45**, 5752 (1992).

[36] A. Balzarotti, M. Cini, E. Perfetto, and G. Stefanucci, J. Phys.: Condens. Matter. **16** R1387R1422 (2004).

[37] W. Langer, M. Plischke and D. M. Mattis, Phys. Rev Lett. **23**, 1448 (1969).

[38] M. Cyrot, Phys. Rev Lett. **25**, 871 (1970).

[39] X.-J. Chen, V. V. Struzhkin, R. J. Hemley, H.-k. Mao, and C. Kendziora, Phys. Rev. B**70**, 214502 (2004).

[40] T. Yildirim, O. Zhou, J. E. Fischer, N. Bykovetz, R. A. Strongin, M. A. Cichy, A. B. Smith III, C. L. Lin and R. Jelinek, Nature **360**, 568 - 571 (1992).